HHS Public Access

Author manuscript

Dev Biol. Author manuscript; available in PMC 2017 January 01.

Published in final edited form as:

Dev Biol. 2016 January 1; 409(1): 202–217. doi:10.1016/j.ydbio.2015.10.023.

PTEN is required to maintain luminal epithelial homeostasis and integrity in the adult mammary gland

Amy N. Shore[a,*], **Chi-Hsuan Chang**[b], **Oh-Joon Kwon**[a], **Matthew C. Weston**[c], **Mei Zhang**[d], **Li Xin**[a], and **Jeffrey M. Rosen**[a]

[a]Department of Molecular and Cellular Biology, Baylor College of Medicine, One Baylor Plaza, Houston, TX, 77030, USA

[b]Integrative Molecular and Biomedical Sciences Graduate Program, Baylor College of Medicine, Houston, TX 77030, USA

[c]The Cain Foundation Laboratories, The Jan and Dan Duncan Neurological Research Institute, Department of Pediatrics, Baylor College of Medicine, Houston, TX, 77030, USA

[d]Department of Developmental Biology, University of Pittsburg, Pittsburg, PA, 15213, USA

Abstract

In the mammary gland, PTEN loss in luminal and basal epithelial cells results in differentiation defects and enhanced proliferation, leading to the formation of tumors with basal epithelial characteristics. In breast cancer, PTEN loss is associated with a hormone receptor-negative, basal-like subtype that is thought to originate in a luminal epithelial cell. Here, we show that luminal-specific PTEN loss results in distinct effects on epithelial homeostasis and mammary tumor formation. Luminal PTEN loss increased proliferation of hormone receptor-negative cells, thereby decreasing the percentage of hormone receptor-positive cells. Moreover, luminal PTEN loss led to misoriented cell divisions and mislocalization of cells to the intraluminal space of mammary ducts. Despite their elevated levels of activated AKT, *Pten*-null intraluminal cells showed increased levels of apoptosis. One year after *Pten* deletion, the ducts had cleared and no palpable mammary tumors were detected. These data establish PTEN as a critical regulator of luminal epithelial homeostasis and integrity in the adult mammary gland, and further show that luminal PTEN loss alone is not sufficient to promote the progression of mammary tumorigenesis.

Keywords

epithelial; homeostasis; mammary; PTEN

[*]corresponding author: amy.shore@bcm.edu.

INTRODUCTION

In adult epithelial tissues, the balance between cell division and cell death maintains proper cell numbers, and thus, proper tissue architecture and function, in a process referred to as homeostasis (Datta et al, 2011; Macara et al, 2014; Ragkousi & Gibson, 2014). Epithelial integrity also relies on the maintenance of oriented cell divisions, cell-cell adhesion, and apical-basal polarity, which is defined by the distinct localization of lipids and proteins to the apical or basal domains of a cell. In the adult mammary gland, there is a network of hollow epithelial ducts that carry nutrient-rich milk to offspring during lactation (Fu et al, 2014; Inman et al, 2015; Visvader, 2009). The ducts are comprised of a single, outer layer of basal epithelial cells and a single, inner layer of polarized luminal epithelial cells. The luminal compartment contains hormone receptor-positive cells, which regulate the proliferation of neighboring cells via a paracrine mechanism, and hormone receptor-negative progenitor cells. The epithelium of the adult mammary gland is not only subject to hormonally driven changes in proliferation and apoptosis during each pregnancy, but also during each estrous cycle (Fata et al, 2001). Throughout these dynamic phases, preservation of the simple epithelial structure of the mammary ducts is essential for lactation, and more importantly, it is essential for preventing mammary tumorigenesis (McCaffrey & Macara, 2011).

The tumor suppressor phosphatase and tensin homolog (PTEN) plays a central role in regulating organ growth and development (Manning & Cantley, 2007; Song et al, 2012). PTEN dephosphorylates phosphatidylinositol 3,4,5-triphosphate (PIP3), the product of phosphatidylinositol kinase 3 (PI3K), thereby attenuating the nutrient- and growth factor-sensing PI3K pathway. Loss of PTEN leads to an accumulation of PIP3, which recruits AKT to the plasma membrane. At the plasma membrane, AKT is phosphorylated and activated, and via its regulation of many downstream targets, phosphorylated AKT (pAKT) enhances cell growth, proliferation, and survival. These pAKT-mediated effects following PTEN loss drastically disrupt homeostasis in multiple epithelial tissues, including intestine, skin, mammary gland, and several reproductive tissues, with the most commonly reported phenotypes being increased proliferation and altered differentiation of specific epithelial populations (Knobbe et al, 2008; Langlois et al, 2009; Miyagawa et al, 2015; Xu et al, 2014). However, recent data indicate that PTEN has additional roles in maintaining epithelial integrity. Several *in vitro* models using mammalian epithelial cells have shown that PTEN regulates mitotic spindle orientation, apical polarity, and lumen formation (Feng et al, 2008; Martin-Belmonte et al, 2007; Toyoshima et al, 2007). Importantly, a recent study provided *in vivo* evidence for each of these functions by showing that PTEN loss in prostate luminal epithelial cells results in randomized mitotic spindle orientation, decreased cell-cell adhesion, and disrupted apical polarity (Wang et al, 2014). Interestingly, loss of PTEN in prostate basal epithelial cells does not affect polarity or mitotic spindle orientation, suggesting that these PTEN functions may be cell-context dependent.

In the mammary epithelium, PTEN loss leads to multiple developmental defects. Deletion of *Pten* in both epithelial compartments of the mouse mammary gland using a mouse mammary tumor virus (MMTV)-driven Cre recombinase during puberty results in increased proliferation, hyperbranching of the mammary ducts, and precocious alveolar differentiation

(Li et al, 2002). In adult virgin mice, deletion of *Pten* in luminal and basal epithelial cells also results in a rapid induction of alveolar differentiation, accompanied by milk production (Chen et al, 2012). These studies demonstrate a key role for PTEN in regulating proliferation and alveolar differentiation in mammary epithelium. Interestingly, *in vitro* studies using three dimensional (3D) mammary epithelial culture models have also shown that PTEN is required for lumen formation and apical polarity (Berglund et al, 2013; Fournier et al, 2009). However, the precise effects of PTEN loss on epithelial architecture, including mitotic spindle orientation, cell-cell adhesion, and apical-basal polarity, have not yet been assessed *in vivo*. Furthermore, the distinct effects of PTEN loss in luminal compared with basal epithelial cells, such as those observed in the prostate, have not yet been investigated in the mammary gland.

Because *PTEN* is one of the most frequently mutated genes in cancer, PTEN is best known for its role in tumor suppression. The hyperactivation of AKT that occurs upon loss of PTEN confers essential properties to cancer cells, such as their enhanced proliferative ability and their ability to evade anoikis, which is a type of cell death that occurs as a result of inappropriate cell or extracellular matrix interactions (Buchheit et al, 2014; Guadamillas et al, 2011). In breast cancer, PTEN loss is correlated with an aggressive, hormone receptor-negative, basal-like tumor phenotype (Cancer Genome Atlas, 2012; Marty et al, 2008; Saal et al, 2008; Saal et al, 2005). Consistent with these findings, loss of PTEN in mammary epithelial 3D culture models results in a reduction in hormone receptor expression and an increase in the expression of basal epithelial markers (Ghosh et al, 2013; Korkaya et al, 2009). Furthermore, mammary tumors that arise in mice with *Pten* deletion in luminal and basal epithelial cells express basal-specific keratins, similar to those expressed in human basal-like breast cancer (Li et al, 2002; Saal et al, 2008). Initially, it was hypothesized that basal-like breast tumors originate from basal epithelial cells; however, accumulating data suggest that, for some tumor-initiating mutations, basal-like tumors originate from hormone-receptor negative, luminal progenitor cells (Lim et al, 2009; Molyneux et al, 2010). Thus, it is important to dissect distinct luminal and basal epithelial-specific effects of cancer-initiating mutations, and furthermore, to elucidate how these epithelial subtype-specific responses can ultimately promote or suppress cancer progression in that particular cell type.

In this study, we deleted *Pten* using an inducible, luminal epithelial-specific Cre recombinase to determine the effects of luminal PTEN loss on epithelial homeostasis and architecture in the adult mammary gland. At 12 weeks post-induction, luminal PTEN loss disrupted the architecture of the luminal compartment and resulted in an accumulation of intraluminal epithelial cell clusters. Not surprisingly, luminal PTEN loss led to increased proliferation, and this was accompanied by a reduced percentage of progesterone receptor (PR)-positive cells. Furthermore, loss of PTEN led to misoriented mitotic spindles in luminal epithelial cells, without affecting cell-cell adhesion or apical polarity. Surprisingly, we also observed an increase in apoptosis of the intraluminal cells, suggesting that, in this model of PTEN loss, activated AKT does not confer anoikis resistance. At 1 year post-induction, the majority of intraluminal cells had cleared and the ducts largely resembled those of control mice, indicating that *Pten*-null luminal cells are lost over time. Moreover, although macroscopic lesions were observed using whole mount analysis, no palpable

mammary tumors were detected, suggesting that loss of PTEN in the luminal compartment alone is not sufficient to promote mammary tumorigenesis. Together, these data identify a novel role for the tumor suppressor PTEN in regulating oriented cell divisions in the mammary luminal epithelium, and demonstrate the necessity for PTEN in maintaining luminal epithelial cell homeostasis and epithelial integrity in the adult mammary gland. Furthermore, these results indicate that PTEN loss in luminal epithelial cells is not sufficient to confer anoikis resistance; therefore, *Pten*-null luminal cells are unable to sustain lumen filling and promote palpable mammary tumor formation.

MATERIALS AND METHODS

Animal Care

This study was performed in strict accordance with the recommendations in the Guide for the Care and Use of Laboratory Animals of the National Institutes of Health. The animal research protocol was approved by the Institutional Animal Care and Use Committee of Baylor College of Medicine (AN-504). All mice used in this study were maintained and euthanized under the guidelines of the Institutional Animal Care and Use Committee of Baylor College of Medicine. The sources of the mouse lines and the genotyping strategies used for each line were previously described (Choi et al, 2012). Tamoxifen (Sigma-Aldrich, St. Louis, MO) was dissolved into corn oil and was administrated into adult female mice (2 mg/40 g), at 8–12 weeks of age, once a day, for four consecutive days, via intraperitoneal injection.

MEC Isolation and Flow Cytometric Analysis

One week after completion of Tmx treatment (K8mTmG mice), or 12 weeks after Tmx or vehicle treatment (K8-CTR or K8PTEN-KO mice), the third, fourth, and fifth pairs of mammary glands were harvested from virgin female mice. MECs were isolated as previously described (Shore et al, 2012). MECs were resuspended at a concentration of 1×10^8 cells/ml in HBSS supplemented with 10 mM HEPES and 2% FBS (HBSS+). This cell suspension was depleted of lineage-positive cells (CD45, Ter119, CD31, and BP-1) using the EasySep™ Mouse Epithelial Cell Enrichment Kit (Stem Cell Technologies). MECs were subsequently resuspended in HBSS+ at a density of 1×10^7 cells/ml and stained with anti-mouse CD24 conjugated to Allophycocyanin (APC) (Biolegend, 1:100), anti-mouse CD29 conjugated to Pacific Blue (BioLegend, 1:100), and anti-mouse CD49f conjugated to Pacific Blue (Biolegend, 1:100). Cells were analyzed using a BD LSR Fortessa Cell Analyzer. Flow Cytometry data was analyzed using FloJo software.

Tissue Processing

The third and fourth mammary gland pairs were excised from mice and fixed for downstream processing. For immunostaining, mammary glands were fixed in 4% paraformaldehyde (PFA) at room temperature for 4 hr or at 4ºC overnight, and then transferred to 70% ethanol, prior to embedding in paraffin. Alternatively, glands were processed for whole mount staining, as described below, prior to embedding in paraffin. Five micron sections were cut using a Shandon Finesse 325 Manual Microtome (Thermo Scientific) and adhered to HistoBond microscope slides (VWR).

H&E and Masson's Trichrome Staining

Tissue sections from Carnoy's fixed glands were deparaffinized and rehydrated through a series of ethanols, and then stained with H&E or Masson's trichrome as described previously (https://www.bcm.edu/research/labs/jeffrey-rosen/protocols). The stained sections were mounted in Poly-Mount Xylene (Polysciences, Inc) and imaged using an Olympus light microscope (BX40) with an Olympus HIH-035382 camera.

Mammary Gland Whole Mounting

The fourth pair of mammary glands were harvested from mice and spread onto glass slides. Next, they were fixed in Carnoy's Fix (6:3:1 mixture of 100% ethanol, chloroform, and glacial acetic acid) for 1–4 hr, and stained in carmine-alum stain overnight. The stained glands were washed and dehydrated in 70%, 95%, and 100% ethanol for 1 hr each, and then transferred to xylene overnight for clearing. They were mounted in Poly-Mount Xylene (Polysciences, Inc) and imaged using a Leica MZ16F Stereoscope with a Leica DFC300FX camera.

Branching Analysis

Branches were counted from images of mammary gland whole mounts using ImagePro software. For each gland, the branch points were counted along 4–6 primary ducts. The total number of branch points was divided by the length of each duct (mm). Each point on the graph (Fig. 2C) represents an average of the branch points/mm from the primary ducts of an individual gland.

Immunofluorescence

Tissue sections from Carnoy's fixed glands, or PFA fixed glands for PR and pSTAT5 IF, were deparaffinized in xylene and rehydrated through a series of ethanols. Antigen retrieval was performed by boiling the sections in 10 mM Sodium Citrate buffer at pH=6.0 for 20 min. Alternatively, for PR, pSTAT5, and CC3 IF, sections were boiled in TE buffer (20mM Tris, 1mM EDTA, 0.05% Tween-20 at pH=9.0) for 20 min. Sections were incubated in blocking buffer (5% BSA, 0.5% Tween-20 in PBS) for 1hr, and then in blocking buffer with primary antibody overnight at 4ºC in a humidified chamber. Alternatively, for ZO-1 and aPKC IF, we used PBS with 5% goat serum as the blocking buffer, or for mouse antibodies, we used the Vector M.O.M. Immunodetection Kit (Vector Labs). We used the following antibodies and dilutions: K8 (Developmental Studies Hybridoma Bank, TROMA-1, 1:250), K14 (Covance, PRB-155P, 1:400), GFP (Abcam, ab290, 1:200 or Clontech, 632381, 1:200), pAkt-Ser473 (Cell Signaling, 3787, 1:100), pS6-Ser240/244 (Cell Signaling, 5364, 1:500), K6 (Covance, PRB-169P, 1:200), NKCC1 (a gift from Jim Turner, 1:200), Npt2b (a gift from Jurg Biber, 1:300), pSTAT5 (Cell Signaling, 9314, 1:200), β-casein (a gift from Mina Bissell, 1:100), PR (DAKO, A0098, 1:75), Ki67 (Vector Labs, VP-K451, 1:200), pH3 (Millipore, 06-570, 1:250), E-cad (Cell Signaling, 3195, 1:200), aPKC (Santa Cruz Biotechnology, sc-216, 1:100), pERM (Cell Signaling, 3141, 1:300), ZO-1 (Developmental Studies Hybridoma Bank, R26.4C, 1:50), and CC3 (Cell Signaling, 9661, 1:200). Following primary antibody incubation, sections were incubated with the appropriate secondary antibody conjugated to Alexa-488 or Alexa-594 (Life Technologies, 1:1000) in blocking

buffer for 1 hr at room temperature. Nuclei were counterstained with NucBlue Fixed Cell ReadyProbes Reagent (Life Technologies). Following IF staining, slides were mounted using Aqua Poly/Mount (Polysciences, Inc). For general epifluorescence, images were captured using an Olympus microscope (BX50) with a SPOT 7.4 Slider RTKE camera (Diagnostic Instruments, Inc.). Exposure times were kept constant for each antibody. Confocal images were captured using a Zeiss LSM 710 microscope equipped with 405nM, 488nM, 561nM, 633nM lasers. Confocal images were acquired with a 20x (0.8 NA) lens and identical settings were used for laser intensity, gain, pixel dwell time, and scan area, between groups for each antibody.

Mitotic Spindle Orientation Measurement

The mitotic spindle orientation was measured in cells in anaphase or telophase as described in Figure 5A. The spindle angles were measured from 40X IF images using the angle measurement tool in ImageJ. The mitotic events were obtained from at least four mice for each group. Mitotic events were excluded if the ducts lacked a defined lumen or basement membrane, or if the epithelial subtype was not discernable.

TUNEL Assay

TUNEL staining was performed using sections from Carnoy's fixed mammary glands as described previously (https://www.bcm.edu/research/labs/jeffrey-rosen/protocols).

Image Processing and Analysis

For each IF experiment, the brightness and contrast of the K8PTEN-KO and K8-CTR images were equally adjusted using Adobe Photoshop. Image quantification was performed manually using ImagePro software. For each mouse or mammary gland, at least 1,000 cells were counted from 6–10 random, 40× images.

Statistics

One-way ANOVA, followed by a Tukey post-test, was performed for all experiments involving three or more groups. Unpaired Student *t*-tests were performed for experiments with only two groups. The graphs in each figure are labeled with p-values, unless the differences were not significant. The number of mice (n) used for each experiment is also indicated on each graph or table. For some experiments, the n indicates another variable that is defined in the figure legend or table.

RESULTS

K8mTmG mice exhibit robust and specific Cre recombinase activity in the luminal mammary epithelium

To delete *Pten* specifically in the luminal compartment of the mammary epithelium, we used an inducible, bacterial artificial chromosome (BAC) transgenic mouse model, K8-CreER^{T2}, in which the regulatory regions of the luminal epithelial-specific gene keratin 8 (*K8*) drive the expression of the CreER^{T2} transgene (Zhang et al, 2012). CreER^{T2} encodes a Cre recombinase that is fused to a mutant estrogen ligand binding domain, allowing the Cre to

become active only in the presence of tamoxifen (Tmx). To determine the efficiency and specificity of the K8-CreER^{T2} transgene in the mammary gland, we bred K8-CreER^{T2} mice to mT/mG reporter mice (K8-CreER^{T2}; mT/mG, or K8mTmG). The mT/mG mouse line ubiquitously expresses a membrane-targeted, tandem-dimer (td) Tomato fluorescent protein (mT) in the absence of Cre activity (Muzumdar et al, 2007). In the presence of Cre activity, the loxP-flanked mT gene is excised and a membrane-targeted green fluorescent protein (mG) is expressed. Because our primary goal was to understand the role of PTEN in regulating adult mammary epithelial homeostasis, we treated 8- to 10-week-old K8mTmG female mice with 2mg/40g Tmx (+Tmx) in corn oil, or corn oil alone (+vehicle), once daily, for four consecutive days. One week after the end of treatment, mice were separated into two groups to perform fluorescence-activated cell sorting (FACS) analysis of isolated mammary epithelial cells (MECs) or immunofluorescence (IF) of paraformaldehyde (PFA)-fixed mammary glands.

The mammary epithelium of freshly harvested mammary glands from the vehicle-treated mice showed no evidence of mG expression using a fluorescent stereoscope, whereas the mammary ducts of the Tmx-treated mice showed robust mG expression (Fig. 1A). For FACS analysis, we first analyzed MECs by their endogenous expression of mT and mG. In the vehicle-treated control K8mTmG mice, 100% of the MEC population was mT-positive, whereas no mG-positive MECs were detected, verifying that the Cre recombinase is active only in the presence of Tmx. In the Tmx-treated K8mTmG mice, 93.9% of the MEC population still expressed the mT protein, likely due to the long half-life of the mT protein (Muzumdar et al, 2007), but showed reduced mT signal intensity compared with the vehicle-treated control MECs (Supp. Fig. 1), and 63.9% expressed the mG protein.

Next, the mT- and mG-positive populations were each analyzed by FACS using anti-CD24 and -CD29 fluorescent-conjugated antibodies to separate the epithelial cells into luminal (CD24^{hi}CD29^{lo}) and basal (CD24^{lo}CD29^{hi}) cell subpopulations (Fig. 1B). Among the luminal population from the Tmx-treated K8mTmG mice, 93.8% were mG-positive, demonstrating robust expression and activation of the K8-driven Cre recombinase in the mammary luminal epithelium. Although the FACS analysis showed that the Cre activity was largely confined to the luminal compartment, we found that 2.2% of the basal population was also mG-positive. Interestingly, previous studies using K8 promoter-driven Cre to induce fluorescent reporter expression in luminal cells also identified a small percentage of fluorescence-positive cells in the basal compartment by FACS analysis (Tao et al, 2014; Van Keymeulen et al, 2011), suggesting that this K8-CreER^{T2} activity in the basal epithelium is specific.

We performed IF to further validate and quantify the efficiency and specificity of the K8-CreER^{T2} transgene in the mammary gland (Fig. 1C). We used antibodies to keratin 8 (K8) to detect the luminal epithelial cells or to keratin 14 (K14) to detect the basal epithelial cells, and to green fluorescence protein (GFP) to detect the mG-positive cells. We quantified the co-localization of GFP with each epithelial marker and found that 92.73% of the K8-positive cells, and 2.72% of the K14-positive cells, were GFP-positive by IF, similar to the percentages that we observed by FACs analysis. In summary, the K8-CreER^{T2} mouse line

generated by BAC transgenesis drives efficient and specific recombination in the luminal epithelium of the mouse mammary gland.

Luminal PTEN loss disrupts lumen maintenance and epithelial architecture within the mammary ducts

To determine the effects of luminal loss of PTEN on adult mammary epithelial cell homeostasis, we bred K8-CreER^{T2} mice to *Pten*$^{fl/fl}$ mice and treated them with Tmx [K8-CreER^{T2}; *Pten*$^{fl/fl}$ (+Tmx), or K8PTEN-KO] at 8 to 12 weeks of age, as described above. As controls, littermates were treated with corn oil alone [K8-CreER^{T2}; *Pten*$^{fl/fl}$ (+vehicle), or K8-CTR-Veh], and K8-CreER^{T2} mice with wild-type *Pten* alleles were treated with Tmx [K8-CreER^{T2}; *Pten*$^{+/+}$ (+Tmx), or K8-CTR-Tmx]. We harvested the mammary glands 12 weeks after treatment to examine potential phenotypic effects of PTEN loss (Fig. 2A illustrates the experimental design). At the whole mount level, the mammary glands from K8PTEN-KO mice appeared similar to those of control mice (Fig. 2B, top three images), and branching quantification confirmed that there were no significant differences among the treatment groups (Fig. 2C). Thus, unlike the ductal hyperbranching that is induced following loss of PTEN in both luminal and basal epithelial cells during puberty (Li et al, 2002), luminal loss of PTEN at 8 to 12 weeks of age did not affect branching morphogenesis.

Next, we analyzed hematoxylin and eosin (H&E)-stained mammary gland sections to detect histological abnormalities. The ducts from control mice had a single layer of luminal epithelial cells surrounded by a single layer of basal epithelial cells, whereas the ducts from K8PTEN-KO mice contained clusters of epithelial cells protruding into the lumen (Fig. 2B, bottom three images), suggesting that PTEN is required to maintain the normal epithelial structure of the luminal compartment. Quantification showed that more than 80% of the mammary ducts from K8PTEN-KO mice contained epithelial protrusions in their lumens, verifying the penetrance of *Pten* deletion and the robustness of the resulting phenotypic consequences (Fig. 2D). Because there were no observable differences between the control groups, for the remainder of this manuscript, the controls are represented as a single group, referred to as K8-CTR. However, all experiments were performed using both control groups, and the quantitative data for each group were analyzed individually to determine that there were no significant differences between the groups prior to combining the data (Supp. Table 1).

To demonstrate efficient K8-driven Cre recombination at the *Pten* allele, prior to further phenotypic analysis, we performed IF using antibodies to two well-characterized downstream targets of the mTOR pathway that are increased upon loss of PTEN: pAKT (Ser 473) and pS6 (Ser 240/244). As expected, levels of pAKT and pS6 were increased in luminal epithelial cells throughout the K8PTEN-KO mammary ducts compared with their respective levels in the control ducts (Fig. 3A), demonstrating robust activation of the mTOR pathway as a result of PTEN loss.

Next, we performed IF using antibodies to K8 and K14 to determine which cell type constituted the intraluminal cell clusters in the K8PTEN-KO ducts. The K8-CTR ducts showed single layers of K8-positive luminal cells and K14-positive basal cells, whereas the K8PTEN-KO ducts had multiple layers of K8-positive luminal cells protruding into the

lumen, surrounded by a single layer of K14-positive basal cells (Fig. 3B), verifying that PTEN loss resulted in an expansion of the luminal compartment. Previous studies have shown that PTEN loss in mammary epithelial cells leads to increased expression of keratin 6 (K6) (Korkaya et al, 2009; Li et al, 2002), a keratin that is normally highly expressed in luminal cells during embryonic and pubertal development (Grimm et al, 2006). In the adult mammary gland, K6 is expressed at very low levels in a small subset of K8/hormone receptor-positive cells that have been shown to possess progenitor-like characteristics (Bu et al, 2011; Grimm et al, 2006; Stingl et al, 2006). To determine if K6 expression is induced in the K8PTEN-KO mammary ducts, we performed IF and found that it was highly increased in luminal epithelial cells of K8PTEN-KO mice compared with those of control mice, particularly in the cells protruding into the lumen (Fig. 3B), suggesting that PTEN loss alters the differentiation state of luminal epithelial cells.

To further investigate the effect of PTEN loss on differentiation of the mammary epithelium, we performed FACS using anti-CD24 and -CD29 antibodies to analyze the luminal and basal epithelial populations. MECs isolated from K8-CTR mice were distributed into the characteristic subpopulations; however, surprisingly, MECs from K8PTEN-KO mice failed to separate into readily distinguishable subpopulations (Fig. 3C). The altered CD24/CD29 profile of the K8PTEN-KO MECs appeared to be largely due to a lack of separation using the anti-CD29 antibody (Supp. Fig. 2), which recognizes β1 integrin, suggesting that luminal PTEN loss disrupts β1 integrin expression. The profile using the anti-CD24 antibody, which recognizes a cell surface, GPI-linked protein involved in cell adhesion, was also altered in the MECs from K8PTEN-KO mice, but to a lesser degree. To determine whether this effect would be observed using another cell surface marker, we performed FACS using an antibody to CD24 in combination with an antibody to CD49f, which recognizes integrin alpha 6. Interestingly, using these antibodies, the MECs from K8PTEN-KO mice sorted into distinct luminal and basal subpopulations; however they did appear to be shifted relative to those of the K8-CTR control mice (Supp. Fig. 3). These data further demonstrate that luminal PTEN loss not only disrupted mammary ductal architecture, it also altered the expression of defining cell surface markers in mammary epithelial subpopulations.

Previous studies have shown that MMTV-driven deletion of *Pten* in both epithelial compartments of virgin mice results in precocious alveolar differentiation of mammary epithelial cells (Chen et al, 2012; Li et al, 2002). To investigate whether luminal loss of PTEN in K8PTEN-KO adult virgin mice leads to precocious alveolar differentiation, we performed IF using antibodies to well-characterized mammary differentiation markers. Interestingly, we observed only minor alterations in the levels of Na-K-Cl co-transporter 1 (NKCC1), which is normally expressed in the majority of luminal epithelial cells of the adult virgin mammary gland, and the Na-Pi co-transporter isoform Npt2b, which is normally induced on the apical surface of luminal MECs during late pregnancy and early lactation, in the K8PTEN-KO ducts (Supp. Fig. 4). Importantly, in the K8PTEN-KO ducts, we did not detect activated phospho-STAT5, a major transcriptional regulator of alveologenesis, or the milk protein β-casein, both of which are detected in mammary epithelium following deletion of *Pten* using MMTV-Cre. Taken together, these data suggest that luminal PTEN loss alone is not sufficient to induce precocious alveolar differentiation in virgin mice.

Luminal PTEN loss increases proliferation and disrupts PR expression and patterning in the luminal epithelium

A previous study showed that MMTV-driven deletion of *Pten* in the mammary gland increases proliferation of MECs (Li et al, 2002). To detect alterations in proliferation, we performed IF using antibodies to the mitotic marker phosphorylated histone H3 at serine 10 (pH3) and to the active cell cycle marker Ki67. A 2.4-fold increase in pH3-positive, and a 3.6-fold increase in Ki67-positive, cells was observed in the K8PTEN-KO ducts compared with the K8-CTR ducts (Fig. 4A), indicating that PTEN is required to maintain luminal epithelial cells in a quiescent state in the adult mammary gland.

In the mature mammary gland, epithelial proliferation is largely regulated by hormone receptor-positive cells via a paracrine mechanism, and the hormone receptor-positive cells themselves rarely proliferate (Brisken & O'Malley, 2010; Brisken et al, 1998; Clarke et al, 1997; Mallepell et al, 2006; Seagroves et al, 2000). To investigate whether PTEN loss induces proliferation in progesterone receptor (PR)-expressing cells, we performed IF on serial sections using antibodies to PR and Ki67. In the K8PTEN-KO ducts, the PR-positive cells largely localized to the intraluminal space and the Ki67-positive cells largely localized to the luminal cells contacting the basal cells, and the two populations did not appear to overlap (Fig. 4B). These data suggest that PTEN loss is only able to induce proliferation of PR-negative cells.

Previous studies have shown that loss of PTEN in mammary epithelial cells results in decreased hormone receptor expression *in vitro* (Ghosh et al, 2013; Korkaya et al, 2009). To determine whether luminal loss of PTEN affects hormone receptor expression or patterning *in vivo*, we performed IF to detect and quantify PR. Quantification showed that in the K8-CTR ducts, 39% of the luminal epithelium was PR positive, whereas in the K8PTEN-KO ducts, only 24% of the luminal epithelium was PR positive (Fig. 4C). Furthermore, in the K8-CTR ducts, PR was expressed in a uniform pattern throughout the luminal epithelium (Fig. 4C). However, in the K8PTEN-KO ducts, less than 10% of the luminal cells that were in direct contact with the basal cells expressed PR, whereas almost 50% of the intraluminal cells expressed PR (Fig. 4D). These data demonstrate that luminal loss of PTEN not only reduced the overall level, it also disrupted the patterning, of PR expression in the ductal epithelium.

The observed differential effects of PTEN loss on hormone receptor-positive and -negative luminal epithelium could have several explanations. It could be the result of biased recombination at the *Pten* allele in PR-negative epithelial cells. However, we demonstrated that the K8-driven Cre is capable of inducing recombination in more than 90% of luminal epithelial cells (Fig. 1), and we observed high levels of pAKT and pS6 in populations of PR-expressing cells (Supp. Fig. 5A and B). These data suggest that *Pten* is deleted in both the PR-positive and -negative epithelium. Alternatively, the alterations in the overall levels of PR-expressing cells in the K8PTEN-KO ducts could be due to a reduction in the PR-positive cell population or an expansion of the PR-negative cell population. Simple quantification of the epithelial cell types showed that although there was a 2-fold increase in overall epithelial cell number in the K8PTEN-KO ducts compared with the K8-CTR ducts, there was only a

1.2-fold increase in PR-positive epithelial cells (Fig. 4E). These results, combined with the lack of co-localization of PR and Ki67 (Fig. 4B), indicate that luminal PTEN loss leads to a preferential expansion of the PR-negative epithelial population and reveal a potential mechanism for the PR-negative phenotype of breast tumors that is associated with PTEN loss.

Loss of PTEN randomizes the orientation of luminal epithelial cell division without disrupting cell-cell adhesion or apical polarity

Misoriented cell divisions could contribute to the luminal filling phenotype we observed, and previous studies have shown that loss of PTEN disrupts the mitotic spindle orientation in dividing epithelial cells (Toyoshima et al, 2007; Wang et al, 2014). To determine whether luminal PTEN loss affects mitotic spindle orientation in our model, we performed IF using an antibody to Ki67 or pH3, combined with an antibody to K14 or K8 to identify dividing basal and luminal cells, respectively. We measured the mitotic spindle orientation of cells in anaphase or telophase as shown in Figure 5A. In basal epithelial cells, almost all of the mitotic spindle axes were parallel to the basement membrane (spindle angle < 15º) in the K8-CTR and K8PTEN-KO ducts, demonstrating that luminal PTEN loss did not affect spindle orientation in the basal epithelium (Fig. 5B). In the luminal compartment of the K8-CTR ducts, the majority of dividing epithelial cells also had their mitotic spindle axes parallel to the basement membrane. However, in the luminal epithelial cells of the K8PTEN-KO ducts, the average spindle angle was 4-fold greater than that of the K8-CTR luminal epithelium.

Because many of the mitotic cells in the K8PTEN-KO ducts were in multi-layered regions, we were concerned that the mitotic spindle phenotype could simply be a consequence of the disorganized epithelium, rather than being a direct consequence of PTEN loss. Therefore, we measured the mitotic spindle angles in luminal cells of the single-layered and multi-layered regions of the K8PTEN-KO ducts separately. In the K8-CTR ducts, 81.3% of the luminal epithelial cells had parallel mitotic spindle axes, whereas in the K8PTEN-KO ducts, only 47.1% of the single-layered luminal epithelial cells had parallel mitotic spindle axes, indicating that PTEN loss itself disrupts mitotic spindle orientation (Fig. 5C). In the multi-layered regions of the K8PTEN-KO ducts, there was an even greater reduction in parallel mitotic spindle axes observed (12.7%), demonstrating that the mitotic spindle orientation defects were exacerbated in the multilayered epithelium. Taken together, these data suggest that luminal PTEN loss disrupts mitotic spindle orientation, which likely contributes to the mislocalization of cells to the intraluminal space of the K8PTEN-KO ducts.

Defects in epithelial cell mitotic spindle orientation are often accompanied by alterations in cell-cell adhesion and apical-basal polarity, both of which are critical for maintaining the structure and function of epithelial tissues. Furthermore, in *Pten*-null prostate luminal epithelium, not only are there mitotic spindle orientation defects, but there is also a reduction in the expression of polarity markers and adhesion proteins (Wang et al, 2014). Interestingly, in mammary epithelium, PTEN is required for the formation, but not the maintenance, of cell-cell adhesion and apical polarity in 3D structures *in vitro* (Berglund et al, 2013). To determine whether PTEN loss affects cell-cell adhesion *in vivo*, we analyzed

expression of the cell membrane-localized, adhesion protein E-cadherin by IF, and we found no apparent differences between the K8PTEN-KO and K8-CTR ducts (Fig. 5D). To investigate whether loss of PTEN results in polarity defects, we performed IF with antibodies to the following apically-localized proteins: atypical protein kinase C (aPKC), phospho-ezrin-radixin-moesin (pERM), and zona occludens 1 (ZO-1). There were no observable differences in the levels or localization of these apical polarity markers between the K8PTEN-KO and K8-CTR ducts (Fig. 5D and Supp. Fig. 6), indicating that, similar to previous *in vitro* observations, PTEN is not required to maintain cell-cell adhesion or apical-basal polarity of luminal mammary epithelial cells. Furthermore, these data suggest that the role of PTEN in mitotic spindle orientation in luminal mammary epithelium is independent of cell-cell adhesion and apical-basal polarity.

K8PTEN-KO ducts show increased intraluminal apoptosis

Activated AKT, downstream of PTEN loss, promotes cell survival by inhibiting several pro-apoptotic proteins (Manning & Cantley, 2007). Accordingly, MMTV-driven deletion of *Pten* enhances survival of MECs during early involution in the mammary gland (Li et al, 2002), a process during which differentiated MECs undergo apoptosis following cessation of lactation. However, loss of PTEN in the MMTV-Cre model does not affect levels of apoptosis in the virgin mammary gland. To determine the level of apoptosis in the K8PTEN-KO ducts, we performed IF using an antibody to cleaved caspase-3 (CC3) and terminal deoxynucleotidyl transferase dUTP nick-end labeling (TUNEL) assays. Unexpectedly, we found a 4.3-fold increase in CC3-positive, and a 4.9-fold increase in TUNEL-positive, cells in the K8PTEN-KO ducts compared with the K8-CTR ducts (Fig. 6A and B), suggesting that the proliferation induced by loss of PTEN is counterbalanced by an increase in apoptosis of luminal epithelial cells.

Because activated AKT is strongly associated with enhanced cell survival, we hypothesized that the increased cell death was not a direct consequence of PTEN loss, but was instead due to anoikis of the mislocalized intraluminal cells in the K8PTEN-KO ducts. Anoikis is cell death that occurs as a result of inappropriate cell or extracellular matrix interactions, and has been proposed to be a mechanism for mammary lumen formation and maintenance (Mailleux et al, 2008). To determine whether the increased apoptosis was occurring in intraluminal cells, we quantified the localization of the CC3- and TUNEL-positive cells in the ducts. Luminal cells that were not in direct contact with a basal cell were considered intraluminal, whereas luminal cells that were part of a multi-layered region, but still contacting basal cells, were considered luminal. CC3 staining showed that the increased apoptosis in the K8PTEN-KO ducts occurred exclusively in the intraluminal cells, and there were no increases in apoptosis in the basal or luminal compartments (Fig. 6C). TUNEL staining showed that 81% of the increased apoptosis occurred in the intraluminal compartment, but there was also an increase in apoptosis in the luminal cells. TUNEL staining does not distinguish between apoptotic and necrotic cells; therefore, the differences between the findings using CC3 and TUNEL may be due to an increase in necrosis in the K8PTEN-KO ducts. Together, these data indicate that although the intraluminal cells of the K8PTEN-KO ducts express high levels of the pro-survival factor pAKT, they are not resistant to apoptosis, and they are likely dying due to anoikis.

One year post-Tmx treatment, K8PTEN-KO ducts appear similar to control ducts and show little evidence of hyperactive mTOR signaling

Given the robust phenotypic consequences of hyperactivation of the mTOR signaling pathway in the mammary luminal epithelium that we observed at 12 weeks post-Tmx treatment, we next investigated the long-term effects of luminal PTEN loss. Specifically, we were interested in determining how the increase in proliferation and apoptosis in the luminal compartment at 12 weeks post-Tmx treatment ultimately affected the homeostatic balance in the K8PTEN-KO ducts over time.

To determine the long-term consequences of luminal PTEN loss, we Tmx-treated mice at 10 to 12 weeks of age and removed the mammary glands 1 year later [K8-CreER^{T2}; *Pten*$^{fl/fl}$ (+Tmx), or K8PTEN-KO-1YR]. As a control, we treated littermates with corn oil alone [K8-CreER^{T2}; *Pten*$^{fl/fl}$ (+vehicle), or K8-CTR-1YR]. At 1 year post-Tmx treatment, the overall ductal structures of K8PTEN-KO-1YR mice appeared very similar to those of K8-CTR-1YR mice, at the whole mount level (Fig. 7A). Surprisingly, even by H&E staining, the K8PTEN-KO-1YR ducts were indistinguishable from the K8-CTR-1YR control ducts (Fig. 7A). The majority of the K8PTEN-KO-1YR ducts had a single layer of K8-positive cells contained within a single layer of K14-positive cells (Fig. 7A). Moreover, the K8PTEN-KO-1YR ducts lacked detectable levels of pAKT (Fig. 7A) and pS6 (Supp. Fig. 7), suggesting little, if any, evidence of mTOR hyperactivation. Next, we wanted to determine whether the effects on proliferation and apoptosis were similarly abrogated at this time point. By IF, there were no differences in proliferation, as assessed by Ki67, or apoptosis, as assessed by TUNEL, between the K8PTEN-KO-1YR and K8-CTR-1YR ducts (Fig. 7B). Together, these results suggest that the *Pten*-null luminal epithelial population is largely absent 1 year after Tmx treatment.

Luminal loss of PTEN results in lesions that fail to progress to palpable tumors 1 year post-Tmx treatment

In MMTV-Cre; *Pten*$^{fl/fl}$ mice, mammary tumors are detected as early as 2 months of age (Li et al, 2002), and 83% of mice with heterozygous inactivation of the *Pten* allele develop mammary tumors by 50–66 weeks of age (Stambolic et al, 2000). In the current study, there were no palpable mammary tumors detected at 12 weeks post-Tmx treatment. However, whole mount analysis revealed small ductal lesions in the mammary glands of two out of eight K8PTEN-KO mice, whereas no lesions were detected in K8-CTR mice (n=9) (Supp. Fig. 8). Histological analyses of these lesions by H&E and Masson's trichrome staining, and IF staining to detect K8 and K14, showed fairly normal ductal structures that were largely comprised of collagen-rich stroma.

Moreover, at 1 year post-Tmx treatment, there were no palpable tumors detected in K8PTEN-KO-1YR mice. However, we observed macroscopic mammary lesions in four out of five mice, whereas no lesions were detected in K8-CTR-1YR mice (n=5). The lesions in K8PTEN-KO-1YR mice were larger and more epithelial-rich compared with the mammary lesions observed at 12 weeks post-Tmx treatment (Fig. 7C). Interestingly, the lesions were comprised predominantly of K14-positive cells, rather than K8-positive cells. Furthermore, IF on serial sections indicated that pAKT-positive cells in the lesions overlapped with K14-

positive cells and not with K8-positive cells. These results suggest that these lesions may have arisen from K8-driven Cre recombination at the *Pten* allele in K14-positive cells, potentially from the same small K14/mG-positive population that we observed in K8mTmG reporter mice (Fig. 1C). Furthermore, these data indicate that after 1 year, luminal loss of PTEN induced by K8-driven Cre recombination is not sufficient to promote the progression of mammary tumorigenesis.

DISCUSSION

Previous studies showed that loss of PTEN in both epithelial compartments of mammary ducts results in increased proliferation and branching, precocious alveolar differentiation, and eventually, the formation of mammary tumors (Chen et al, 2012; Li et al, 2002). In this study, we showed that even though luminal epithelial-specific deletion of *Pten* increased proliferation, it was not sufficient to alter branching morphogenesis or induce precocious alveolar differentiation, nor was it sufficient to induce mammary tumor formation. Interestingly, the increased proliferation was accompanied by a reduction in the percentage of PR-positive cells, which was previously only observed using *in vitro* models. Furthermore, the dividing luminal epithelial cells had misoriented mitotic spindles, likely contributing to the observed intraluminal clusters in the ducts of K8PTEN-KO mice. Surprisingly, luminal PTEN loss also led to an increase in apoptosis specifically in the intraluminal cells, suggesting that these cells are likely dying due to anoikis. Finally, 1 year after deletion of *Pten* from the mammary luminal epithelial compartment, the K8PTEN-KO-1YR ducts were indistinguishable from control ducts and showed little evidence of PTEN loss, suggesting that *Pten*-null cells are lost over time. Together, these data suggest that PTEN is essential in the luminal epithelial compartment for maintaining homeostasis and proper ductal architecture in the adult mammary gland. Moreover, these data demonstrate that high levels of pAKT fail to confer anoikis resistance to the *Pten*-null intraluminal clusters; therefore, luminal PTEN loss is not sufficient for evading anoikis and promoting tumor progression.

PTEN loss and PR

Loss of PTEN protein expression is associated with hormone receptor-negative breast cancer (Saal et al, 2005), and *in vitro* studies using human and mouse mammary epithelial 3D culture models have shown that depletion of PTEN leads to a reduction in hormone receptor-positive cells (Ghosh et al, 2013; Korkaya et al, 2009). However, mechanisms that regulate these correlative observations between PTEN and hormone receptor-positive cells are not known. In breast cancer cell lines, it has been shown that growth factor signaling through the PI3K/AKT pathway inhibits *PR* expression, resulting in reduced PR protein levels; however, this mechanism has not been shown to occur downstream of PTEN loss (Cui et al, 2003).

Importantly, in this study, we provided *in vivo* evidence for a reduction in the percentage of PR-positive cells following PTEN loss in the luminal compartment of the adult mammary gland. Furthermore, we showed that the increased proliferation that occurred as a result of PTEN loss appeared to be largely localized to the PR-negative luminal progenitor cells. In

the adult mammary gland, transforming growth factor-β (TGFβ), a potent inhibitor of proliferation, prevents the hormone receptor-positive cells from dividing (Ewan et al, 2005). In some cell types, hyperactivated AKT has been shown to modulate signaling downstream of TGFβ, thereby blunting its anti-proliferative function (Conery et al, 2004; Remy et al, 2004; Seoane et al, 2004). However, our data suggest that the increased levels of pAKT following PTEN loss in luminal mammary epithelium may not be sufficient to overcome the anti-proliferative TGFβ signal in PR positive-cells; therefore, only the PR-negative cells proliferate and expand, resulting in a reduced percentage of PR-positive cells. This potential mechanism of reduced PR expression following PTEN loss in the mammary gland may have significant implications for understanding the role of PTEN loss in dictating breast tumor phenotypes.

Interestingly, PTEN luminal loss also led to a reduction of PR-expressing cells directly contacting the basal epithelial compartment, accompanied by an accumulation of PR-expressing cells in the intraluminal space. The intraluminal cell clusters also expressed increased levels of K6, which is normally expressed in a small population of hormone receptor-positive cells with progenitor activity (Bu et al, 2011; Grimm et al, 2006; Stingl et al, 2006). These data indicate that luminal PTEN loss increases the fraction of hormone receptor-positive luminal progenitors; however, *in vitro* and *in vivo* functional assays will need to be performed to determine whether these intraluminal cells actually possess progenitor activity. Furthermore, the mechanisms responsible for this altered differentiation state following PTEN loss remains to be determined. For instance, their altered differentiation could be the result of the observed perturbations in cell division orientation following PTEN loss, which could lead to alterations in cell fate. Alternatively, their loss of contact with, and signaling from, the basal epithelial compartment and the underlying basement membrane might also affect their differentiation.

PTEN loss and mitotic spindle orientation

Loss of PTEN in our model resulted in clusters of epithelial cells filling the lumen. This is likely due to two effects of PTEN loss: an increase in proliferation and misoriented cell divisions. Furthermore, we show that the mitotic spindle defect is likely a direct result of PTEN loss and a cause of the disorganized epithelium, not simply a consequence. Mitotic spindle orientation defects in epithelia are often accompanied by alterations in cell-cell adhesion and apical-basal polarity (Bergstralh et al, 2013a; Ragkousi & Gibson, 2014). In the prostate gland, luminal loss of PTEN results in misoriented mitotic spindles, and disrupted cell-cell adhesion and apical polarity (Wang et al, 2014). In the present study, luminal PTEN loss resulted in misoriented mitotic spindles without affecting adhesion or apical polarity in the luminal compartment. Consistent with these observations, in *Drosophila* follicular epithelial cells, the lateral polarity factor Discs large (Dlg) is required for spindle orientation of follicular epithelial cells, and this function is independent of its role in apical-basal polarity (Bergstralh et al, 2013b). Additionally, in *Drosophila* epithelia, aurora kinase A (AURKA) is required for regulating mitotic spindle orientation but not cell polarity (Bell et al, 2015). Interestingly, PTEN loss in the prostate epithelium results in increased levels of AURKA and polo-like kinase 1 (PLK1) (Song et al, 2011). PLK1 also has a known role in regulating mitotic spindle orientation in epithelial cells (Kiyomitsu &

Cheeseman, 2012), and furthermore, a recent *in vitro* study showed that PTEN co-localizes with PLK1 at the centrosomes and is required to maintain centrosomal integrity, suggesting there may be a more direct role of PTEN in mitotic spindle orientation (Leonard et al, 2013). These data provide plausible mediators of the spindle orientation defects that we observed downstream of PTEN loss.

Alternatively, β1 integrin has been shown to regulate the mitotic spindle orientation of dividing mammalian epithelial cells *in vitro*, independent of cell-cell adhesion and cell polarity, and this mechanism is dependent on PTEN (Toyoshima et al, 2007; Toyoshima & Nishida, 2007). Other *in vivo* studies have shown a requirement for β1 integrin in mitotic spindle orientation in skin and intestinal epithelia, and in basal epithelial cells of the mammary gland (Chen & Krasnow, 2012; Lechler & Fuchs, 2005; Taddei et al, 2008). Interestingly, we showed that MECs isolated from K8PTEN-KO mammary glands have altered expression of β1 integrin by FACS analysis, thus providing another potential mechanism for the misoriented spindles in the K8PTEN-KO luminal compartment.

PTEN loss and apoptosis

In mammary epithelium, Bcl-2 homology domain 3 (BH3)-only proteins, such as BIM and BMF, are required during anoikis and lumen formation to induce apoptosis (Mailleux et al, 2007; Schmelzle et al, 2007); however, activated AKT has been shown to promote cell survival by blocking these pro-apoptotic proteins. Accordingly, loss of PTEN, or expression of a constitutively active AKT, confers resistance to anoikis in human mammary epithelial cells (Reginato et al, 2003; Vitolo et al, 2009), whereas overexpression of PTEN in breast cancer cells induces anoikis (Lu et al, 1999). In this study, luminal loss of PTEN resulted in the mislocalization of epithelial cells to the intraluminal space. Despite the high levels of pAKT in the K8PTEN-KO intraluminal cells, their apoptotic rates were significantly higher than those in the other epithelial compartments of the K8PTEN-KO and K8-CTR ducts, indicating pAKT is unable to confer anoikis resistance in this model. It is possible that, even though the majority of intraluminal cells expressed high levels of pAKT, there may be a small population of cells with wild-type *Pten* that are dying. Alternatively, the intraluminal cells may be undergoing integrin-mediated death (IMD), an alternative cell death mechanism that involves unligated integrins themselves acting as promoters of caspase 8-mediated apoptosis (Cheresh & Stupack, 2002; Stupack & Cheresh, 2002), which may not be sensitive to pAKT pro-survival signaling. In the K8PTEN-KO ducts, MECs showed alterations in β1 integrin levels, suggesting that the altered integrin profile and mislocalization of the intraluminal cells could both lead to an increase in unligated intregrins and activation of apoptosis through the IMD pathway. Interestingly, a more recent *in vitro* study showed that, in some cell types, hyperactive AKT signaling can actually facilitate cell death mediated by increased levels of reactive oxygen species, demonstrating that pAKT does not always function to promote cell survival (Nogueira et al, 2008).

PTEN loss and mammary tumor formation

PTEN is known to be a potent tumor suppressor. In previously investigated mouse models, PTEN reduction in both epithelial compartments results in mammary tumor formation (Li et al, 2002; Saal et al, 2008; Stambolic et al, 2000). However, in the current study, loss of

PTEN in the majority of luminal epithelial cells failed to result in palpable mammary tumor formation, likely because the increased proliferation following PTEN loss was accompanied by increased apoptosis, ultimately resulting in loss of the *Pten*-null cells. Loss of the *Pten*-null population 1 year after Tmx treatment could also have been due, in part, to exhaustion of the *Pten*-null luminal progenitor pool over time, as *Pten* has been shown to be required to maintain stem and progenitor populations in several adult tissues (Hill & Wu, 2009; Song et al, 2012). Together, these effects following luminal PTEN loss may both contribute to suppression of mammary tumor progression in this model.

PTEN loss is not only associated with one of the more aggressive breast cancer subtypes, it is also associated with resistance to endocrine therapy and receptor tyrosine kinase (RTK) inhibition in breast cancer treatment (Nagata et al, 2004; Tanic et al, 2012). Thus, understanding cellular responses downstream of PTEN loss is critical for designing novel therapeutics to treat patients with basal-like breast tumors, and furthermore, for delineating mechanisms of therapy resistance. The current study identified a novel role for PTEN in regulating proliferation and mitotic spindle orientation to maintain proper organization of the luminal epithelial compartment in the adult mammary gland. Future studies will be required to elucidate the precise mechanisms by which PTEN regulates oriented cell divisions in the luminal epithelium. Moreover, our data suggest that luminal PTEN loss leads to a preferential expansion of the PR-negative luminal progenitor population, which could have important implications for understanding the association of PTEN loss with hormone receptor-negative breast cancer. Our data also showed that high levels of pAKT in the intraluminal cells were, by themselves, not sufficient to confer resistance to apoptosis. It will be critical to delineate the cell death mechanisms used by these cells to suppress tumor initiation following PTEN loss. Finally, our data demonstrate that, 1 year after *Pten* deletion, luminal PTEN loss is not sufficient to promote palpable mammary tumor formation. Thus, future studies should be performed to investigate basal epithelial-specific functions of PTEN, and to determine whether PTEN loss in the basal epithelium shows distinct effects in mammary tumor initiation and progression.

Supplementary Material

Refer to Web version on PubMed Central for supplementary material.

Acknowledgments

We would like to thank Shirley Small for mouse colony maintenance, Maria Gonzalez-Rimbau for tissue sectioning, and Alvenia Daniels for ordering lab supplies. This study was conducted with help from the Cytometry and Cell Sorting Core at Baylor College of Medicine with funding from the NIH (P30 AI036211, P30 CA125123, and S10 RR024574), the Lester and Sue Smith Breast Center Pathology Core, and the Microscopy Core of IDDRC at Baylor College of Medicine (U54 HD083092 from the Eunice Kennedy Shriver National Institute of Child Health & Human Development). The content is solely the responsibility of the authors and does not necessarily represent the official views of the Eunice Kennedy Shriver National Institute of Child Health & Human Development or the National Institutes of Health. ANS, CHC, MZ, and JMR were supported by a grant from the National Cancer Institute (CA016303-39), and MCW was supported by an NINDS K99 Pathway to Independence award (NS087095).

References

Bell GP, Fletcher GC, Brain R, Thompson BJ. Aurora kinases phosphorylate Lgl to induce mitotic spindle orientation in Drosophila epithelia. Curr Biol. 2015; 25:61–68. [PubMed: 25484300]

Berglund FM, Weerasinghe NR, Davidson L, Lim JC, Eickholt BJ, Leslie NR. Disruption of epithelial architecture caused by loss of PTEN or by oncogenic mutant p110alpha/PIK3CA but not by HER2 or mutant AKT1. Oncogene. 2013; 32:4417–4426. [PubMed: 23085752]

Bergstralh DT, Haack T, St Johnston D. Epithelial polarity and spindle orientation: intersecting pathways. Philos Trans R Soc Lond B Biol Sci. 2013a; 368:20130291. [PubMed: 24062590]

Bergstralh DT, Lovegrove HE, St Johnston D. Discs large links spindle orientation to apical-basal polarity in Drosophila epithelia. Curr Biol. 2013b; 23:1707–1712. [PubMed: 23891112]

Brisken C, O'Malley B. Hormone action in the mammary gland. Cold Spring Harb Perspect Biol. 2010; 2:a003178. [PubMed: 20739412]

Brisken C, Park S, Vass T, Lydon JP, O'Malley BW, Weinberg RA. A paracrine role for the epithelial progesterone receptor in mammary gland development. Proc Natl Acad Sci U S A. 1998; 95:5076–5081. [PubMed: 9560231]

Bu W, Chen J, Morrison GD, Huang S, Creighton CJ, Huang J, Chamness GC, Hilsenbeck SG, Roop DR, Leavitt AD, Li Y. Keratin 6a marks mammary bipotential progenitor cells that can give rise to a unique tumor model resembling human normal-like breast cancer. Oncogene. 2011; 30:4399–4409. [PubMed: 21532625]

Buchheit CL, Weigel KJ, Schafer ZT. Cancer cell survival during detachment from the ECM: multiple barriers to tumour progression. Nat Rev Cancer. 2014; 14:632–641. [PubMed: 25098270]

Cancer Genome Atlas N. Comprehensive molecular portraits of human breast tumours. Nature. 2012; 490:61–70. [PubMed: 23000897]

Chen CC, Stairs DB, Boxer RB, Belka GK, Horseman ND, Alvarez JV, Chodosh LA. Autocrine prolactin induced by the Pten-Akt pathway is required for lactation initiation and provides a direct link between the Akt and Stat5 pathways. Genes Dev. 2012; 26:2154–2168. [PubMed: 23028142]

Chen J, Krasnow MA. Integrin Beta 1 suppresses multilayering of a simple epithelium. PLoS One. 2012; 7:e52886. [PubMed: 23285215]

Cheresh DA, Stupack DG. Integrin-mediated death: an explanation of the integrin-knockout phenotype? Nat Med. 2002; 8:193–194. [PubMed: 11875466]

Choi N, Zhang B, Zhang L, Ittmann M, Xin L. Adult murine prostate basal and luminal cells are self-sustained lineages that can both serve as targets for prostate cancer initiation. Cancer Cell. 2012; 21:253–265. [PubMed: 22340597]

Clarke RB, Howell A, Potten CS, Anderson E. Dissociation between steroid receptor expression and cell proliferation in the human breast. Cancer Res. 1997; 57:4987–4991. [PubMed: 9371488]

Conery AR, Cao Y, Thompson EA, Townsend CM Jr, Ko TC, Luo K. Akt interacts directly with Smad3 to regulate the sensitivity to TGF-beta induced apoptosis. Nat Cell Biol. 2004; 6:366–372. [PubMed: 15104092]

Cui X, Zhang P, Deng W, Oesterreich S, Lu Y, Mills GB, Lee AV. Insulin-like growth factor-I inhibits progesterone receptor expression in breast cancer cells via the phosphatidylinositol 3-kinase/Akt/mammalian target of rapamycin pathway: progesterone receptor as a potential indicator of growth factor activity in breast cancer. Mol Endocrinol. 2003; 17:575–588. [PubMed: 12554765]

Datta A, Bryant DM, Mostov KE. Molecular regulation of lumen morphogenesis. Curr Biol. 2011; 21:R126–136. [PubMed: 21300279]

Ewan KB, Oketch-Rabah HA, Ravani SA, Shyamala G, Moses HL, Barcellos-Hoff MH. Proliferation of estrogen receptor-alpha-positive mammary epithelial cells is restrained by transforming growth factor-beta1 in adult mice. Am J Pathol. 2005; 167:409–417. [PubMed: 16049327]

Fata JE, Chaudhary V, Khokha R. Cellular turnover in the mammary gland is correlated with systemic levels of progesterone and not 17beta-estradiol during the estrous cycle. Biol Reprod. 2001; 65:680–688. [PubMed: 11514328]

Feng W, Wu H, Chan LN, Zhang M. Par-3-mediated junctional localization of the lipid phosphatase PTEN is required for cell polarity establishment. J Biol Chem. 2008; 283:23440–23449. [PubMed: 18550519]

Fournier MV, Fata JE, Martin KJ, Yaswen P, Bissell MJ. Interaction of E-cadherin and PTEN regulates morphogenesis and growth arrest in human mammary epithelial cells. Cancer Res. 2009; 69:4545–4552. [PubMed: 19417140]

Fu N, Lindeman GJ, Visvader JE. The mammary stem cell hierarchy. Curr Top Dev Biol. 2014; 107:133–160. [PubMed: 24439805]

Ghosh S, Varela L, Sood A, Park BH, Lotan TL. mTOR signaling feedback modulates mammary epithelial differentiation and restrains invasion downstream of PTEN loss. Cancer Res. 2013; 73:5218–5231. [PubMed: 23774212]

Grimm SL, Bu W, Longley MA, Roop DR, Li Y, Rosen JM. Keratin 6 is not essential for mammary gland development. Breast Cancer Res. 2006; 8:R29. [PubMed: 16790075]

Guadamillas MC, Cerezo A, Del Pozo MA. Overcoming anoikis--pathways to anchorage-independent growth in cancer. J Cell Sci. 2011; 124:3189–3197. [PubMed: 21940791]

Hill R, Wu H. PTEN, stem cells, and cancer stem cells. J Biol Chem. 2009; 284:11755–11759. [PubMed: 19117948]

Inman JL, Robertson C, Mott JD, Bissell MJ. Mammary gland development: cell fate specification, stem cells and the microenvironment. Development. 2015; 142:1028–1042. [PubMed: 25758218]

Kiyomitsu T, Cheeseman IM. Chromosome- and spindle-pole-derived signals generate an intrinsic code for spindle position and orientation. Nat Cell Biol. 2012; 14:311–317. [PubMed: 22327364]

Knobbe CB, Lapin V, Suzuki A, Mak TW. The roles of PTEN in development, physiology and tumorigenesis in mouse models: a tissue-by-tissue survey. Oncogene. 2008; 27:5398–5415. [PubMed: 18794876]

Korkaya H, Paulson A, Charafe-Jauffret E, Ginestier C, Brown M, Dutcher J, Clouthier SG, Wicha MS. Regulation of mammary stem/progenitor cells by PTEN/Akt/beta-catenin signaling. PLoS Biol. 2009; 7:e1000121. [PubMed: 19492080]

Langlois MJ, Roy SA, Auclair BA, Jones C, Boudreau F, Carrier JC, Rivard N, Perreault N. Epithelial phosphatase and tensin homolog regulates intestinal architecture and secretory cell commitment and acts as a modifier gene in neoplasia. FASEB J. 2009; 23:1835–1844. [PubMed: 19168705]

Lechler T, Fuchs E. Asymmetric cell divisions promote stratification and differentiation of mammalian skin. Nature. 2005; 437:275–280. [PubMed: 16094321]

Leonard MK, Hill NT, Bubulya PA, Kadakia MP. The PTEN-Akt pathway impacts the integrity and composition of mitotic centrosomes. Cell Cycle. 2013; 12:1406–1415. [PubMed: 23574721]

Li G, Robinson GW, Lesche R, Martinez-Diaz H, Jiang Z, Rozengurt N, Wagner KU, Wu DC, Lane TF, Liu X, Hennighausen L, Wu H. Conditional loss of PTEN leads to precocious development and neoplasia in the mammary gland. Development. 2002; 129:4159–4170. [PubMed: 12163417]

Lim E, Vaillant F, Wu D, Forrest NC, Pal B, Hart AH, Asselin-Labat ML, Gyorki DE, Ward T, Partanen A, Feleppa F, Huschtscha LI, Thorne HJ, Fox SB, Yan M, French JD, Brown MA, Smyth GK, Visvader JE, Lindeman GJ. kConFab. Aberrant luminal progenitors as the candidate target population for basal tumor development in BRCA1 mutation carriers. Nat Med. 2009; 15:907–913. [PubMed: 19648928]

Lu Y, Lin YZ, LaPushin R, Cuevas B, Fang X, Yu SX, Davies MA, Khan H, Furui T, Mao M, Zinner R, Hung MC, Steck P, Siminovitch K, Mills GB. The PTEN/MMAC1/TEP tumor suppressor gene decreases cell growth and induces apoptosis and anoikis in breast cancer cells. Oncogene. 1999; 18:7034–7045. [PubMed: 10597304]

Macara IG, Guyer R, Richardson G, Huo Y, Ahmed SM. Epithelial homeostasis. Curr Biol. 2014; 24:R815–825. [PubMed: 25202877]

Mailleux AA, Overholtzer M, Brugge JS. Lumen formation during mammary epithelial morphogenesis: insights from in vitro and in vivo models. Cell Cycle. 2008; 7:57–62. [PubMed: 18196964]

Mailleux AA, Overholtzer M, Schmelzle T, Bouillet P, Strasser A, Brugge JS. BIM regulates apoptosis during mammary ductal morphogenesis, and its absence reveals alternative cell death mechanisms. Dev Cell. 2007; 12:221–234. [PubMed: 17276340]

Mallepell S, Krust A, Chambon P, Brisken C. Paracrine signaling through the epithelial estrogen receptor alpha is required for proliferation and morphogenesis in the mammary gland. Proc Natl Acad Sci U S A. 2006; 103:2196–2201. [PubMed: 16452162]

Manning BD, Cantley LC. AKT/PKB signaling: navigating downstream. Cell. 2007; 129:1261–1274. [PubMed: 17604717]

Martin-Belmonte F, Gassama A, Datta A, Yu W, Rescher U, Gerke V, Mostov K. PTEN-mediated apical segregation of phosphoinositides controls epithelial morphogenesis through Cdc42. Cell. 2007; 128:383–397. [PubMed: 17254974]

Marty B, Maire V, Gravier E, Rigaill G, Vincent-Salomon A, Kappler M, Lebigot I, Djelti F, Tourdes A, Gestraud P, Hupe P, Barillot E, Cruzalegui F, Tucker GC, Stern MH, Thiery JP, Hickman JA, Dubois T. Frequent PTEN genomic alterations and activated phosphatidylinositol 3-kinase pathway in basal-like breast cancer cells. Breast Cancer Res. 2008; 10:R101. [PubMed: 19055754]

McCaffrey LM, Macara IG. Epithelial organization, cell polarity and tumorigenesis. Trends Cell Biol. 2011; 21:727–735. [PubMed: 21782440]

Miyagawa S, Sato M, Sudo T, Yamada G, Iguchi T. Unique roles of estrogen-dependent Pten control in epithelial cell homeostasis of mouse vagina. Oncogene. 2015; 34:1035–1043. [PubMed: 24632614]

Molyneux G, Geyer FC, Magnay FA, McCarthy A, Kendrick H, Natrajan R, Mackay A, Grigoriadis A, Tutt A, Ashworth A, Reis-Filho JS, Smalley MJ. BRCA1 basal-like breast cancers originate from luminal epithelial progenitors and not from basal stem cells. Cell Stem Cell. 2010; 7:403–417. [PubMed: 20804975]

Muzumdar MD, Tasic B, Miyamichi K, Li L, Luo L. A global double-fluorescent Cre reporter mouse. Genesis. 2007; 45:593–605. [PubMed: 17868096]

Nagata Y, Lan KH, Zhou X, Tan M, Esteva FJ, Sahin AA, Klos KS, Li P, Monia BP, Nguyen NT, Hortobagyi GN, Hung MC, Yu D. PTEN activation contributes to tumor inhibition by trastuzumab, and loss of PTEN predicts trastuzumab resistance in patients. Cancer Cell. 2004; 6:117–127. [PubMed: 15324695]

Nogueira V, Park Y, Chen CC, Xu PZ, Chen ML, Tonic I, Unterman T, Hay N. Akt determines replicative senescence and oxidative or oncogenic premature senescence and sensitizes cells to oxidative apoptosis. Cancer Cell. 2008; 14:458–470. [PubMed: 19061837]

Ragkousi K, Gibson MC. Cell division and the maintenance of epithelial order. J Cell Biol. 2014; 207:181–188. [PubMed: 25349258]

Reginato MJ, Mills KR, Paulus JK, Lynch DK, Sgroi DC, Debnath J, Muthuswamy SK, Brugge JS. Integrins and EGFR coordinately regulate the pro-apoptotic protein Bim to prevent anoikis. Nat Cell Biol. 2003; 5:733–740. [PubMed: 12844146]

Remy I, Montmarquette A, Michnick SW. PKB/Akt modulates TGF-beta signalling through a direct interaction with Smad3. Nat Cell Biol. 2004; 6:358–365. [PubMed: 15048128]

Saal LH, Gruvberger-Saal SK, Persson C, Lovgren K, Jumppanen M, Staaf J, Jonsson G, Pires MM, Maurer M, Holm K, Koujak S, Subramaniyam S, Vallon-Christersson J, Olsson H, Su T, Memeo L, Ludwig T, Ethier SP, Krogh M, Szabolcs M, Murty VV, Isola J, Hibshoosh H, Parsons R, Borg A. Recurrent gross mutations of the PTEN tumor suppressor gene in breast cancers with deficient DSB repair. Nat Genet. 2008; 40:102–107. [PubMed: 18066063]

Saal LH, Holm K, Maurer M, Memeo L, Su T, Wang X, Yu JS, Malmstrom PO, Mansukhani M, Enoksson J, Hibshoosh H, Borg A, Parsons R. PIK3CA mutations correlate with hormone receptors, node metastasis, and ERBB2, and are mutually exclusive with PTEN loss in human breast carcinoma. Cancer Res. 2005; 65:2554–2559. [PubMed: 15805248]

Schmelzle T, Mailleux AA, Overholtzer M, Carroll JS, Solimini NL, Lightcap ES, Veiby OP, Brugge JS. Functional role and oncogene-regulated expression of the BH3-only factor Bmf in mammary epithelial anoikis and morphogenesis. Proc Natl Acad Sci U S A. 2007; 104:3787–3792. [PubMed: 17360431]

Seagroves TN, Lydon JP, Hovey RC, Vonderhaar BK, Rosen JM. C/EBPbeta (CCAAT/enhancer binding protein) controls cell fate determination during mammary gland development. Mol Endocrinol. 2000; 14:359–368. [PubMed: 10707954]

Seoane J, Le HV, Shen L, Anderson SA, Massague J. Integration of Smad and forkhead pathways in the control of neuroepithelial and glioblastoma cell proliferation. Cell. 2004; 117:211–223. [PubMed: 15084259]

Shore AN, Kabotyanski EB, Roarty K, Smith MA, Zhang Y, Creighton CJ, Dinger ME, Rosen JM. Pregnancy-induced noncoding RNA (PINC) associates with polycomb repressive complex 2 and regulates mammary epithelial differentiation. PLoS Genet. 2012; 8:e1002840. [PubMed: 22911650]

Song MS, Carracedo A, Salmena L, Song SJ, Egia A, Malumbres M, Pandolfi PP. Nuclear PTEN regulates the APC-CDH1 tumor-suppressive complex in a phosphatase-independent manner. Cell. 2011; 144:187–199. [PubMed: 21241890]

Song MS, Salmena L, Pandolfi PP. The functions and regulation of the PTEN tumour suppressor. Nat Rev Mol Cell Biol. 2012; 13:283–296. [PubMed: 22473468]

Stambolic V, Tsao MS, Macpherson D, Suzuki A, Chapman WB, Mak TW. High incidence of breast and endometrial neoplasia resembling human Cowden syndrome in pten+/- mice. Cancer Res. 2000; 60:3605–3611. [PubMed: 10910075]

Stingl J, Eirew P, Ricketson I, Shackleton M, Vaillant F, Choi D, Li HI, Eaves CJ. Purification and unique properties of mammary epithelial stem cells. Nature. 2006; 439:993–997. [PubMed: 16395311]

Stupack DG, Cheresh DA. Get a ligand, get a life: integrins, signaling and cell survival. J Cell Sci. 2002; 115:3729–3738. [PubMed: 12235283]

Taddei I, Deugnier MA, Faraldo MM, Petit V, Bouvard D, Medina D, Fassler R, Thiery JP, Glukhova MA. Beta1 integrin deletion from the basal compartment of the mammary epithelium affects stem cells. Nat Cell Biol. 2008; 10:716–722. [PubMed: 18469806]

Tanic N, Milovanovic Z, Tanic N, Dzodic R, Juranic Z, Susnjar S, Plesinac-Karapandzic V, Tatic S, Dramicanin T, Davidovic R, Dimitrijevic B. The impact of PTEN tumor suppressor gene on acquiring resistance to tamoxifen treatment in breast cancer patients. Cancer Biol Ther. 2012; 13:1165–1174. [PubMed: 22892847]

Tao L, van Bragt MP, Laudadio E, Li Z. Lineage tracing of mammary epithelial cells using cell-type-specific cre-expressing adenoviruses. Stem Cell Reports. 2014; 2:770–779. [PubMed: 24936465]

Toyoshima F, Matsumura S, Morimoto H, Mitsushima M, Nishida E. PtdIns(3,4,5)P3 regulates spindle orientation in adherent cells. Dev Cell. 2007; 13:796–811. [PubMed: 18061563]

Toyoshima F, Nishida E. Integrin-mediated adhesion orients the spindle parallel to the substratum in an EB1- and myosin X-dependent manner. EMBO J. 2007; 26:1487–1498. [PubMed: 17318179]

Van Keymeulen A, Rocha AS, Ousset M, Beck B, Bouvencourt G, Rock J, Sharma N, Dekoninck S, Blanpain C. Distinct stem cells contribute to mammary gland development and maintenance. Nature. 2011; 479:189–193. [PubMed: 21983963]

Visvader JE. Keeping abreast of the mammary epithelial hierarchy and breast tumorigenesis. Genes Dev. 2009; 23:2563–2577. [PubMed: 19933147]

Vitolo MI, Weiss MB, Szmacinski M, Tahir K, Waldman T, Park BH, Martin SS, Weber DJ, Bachman KE. Deletion of PTEN promotes tumorigenic signaling, resistance to anoikis, and altered response to chemotherapeutic agents in human mammary epithelial cells. Cancer Res. 2009; 69:8275–8283. [PubMed: 19843859]

Wang J, Zhu HH, Chu M, Liu Y, Zhang C, Liu G, Yang X, Yang R, Gao WQ. Symmetrical and asymmetrical division analysis provides evidence for a hierarchy of prostate epithelial cell lineages. Nat Commun. 2014; 5:4758. [PubMed: 25163637]

Xu B, Washington AM, Hinton BT. PTEN signaling through RAF1 proto-oncogene serine/threonine kinase (RAF1)/ERK in the epididymis is essential for male fertility. Proc Natl Acad Sci U S A. 2014; 111:18643–18648. [PubMed: 25512490]

Zhang L, Zhang B, Han SJ, Shore AN, Rosen JM, Demayo FJ, Xin L. Targeting CreER(T2) expression to keratin 8-expressing murine simple epithelia using bacterial artificial chromosome transgenesis. Transgenic Res. 2012; 21:1117–1123. [PubMed: 22350718]

Highlights

- PTEN regulates proliferation of mammary luminal epithelial cells.
- PTEN regulates mitotic spindle orientation in mammary luminal epithelial cells.
- PTEN loss in mammary luminal epithelial cells does not confer apoptosis resistance.
- Luminal epithelial PTEN loss is not sufficient to promote mammary tumor progression.

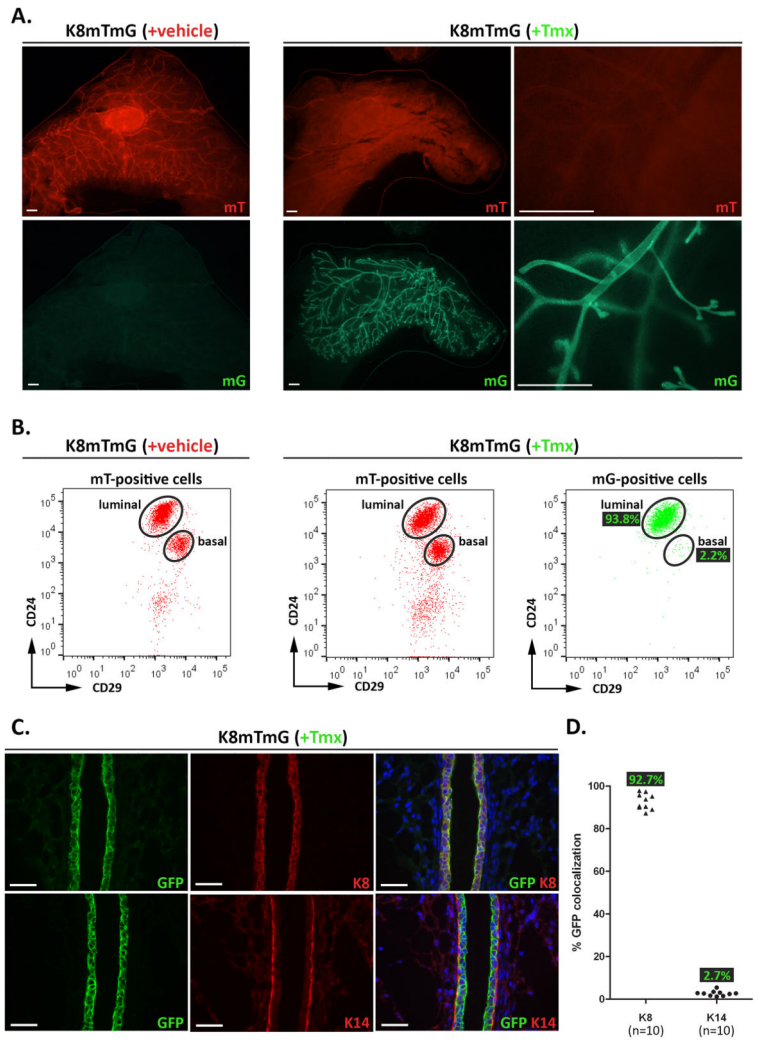

Figure 1. K8mTmG mice exhibit robust and specific Cre recombinase activity in the luminal mammary epithelium

(A–C) K8mTmG mice were treated with vehicle (+vehicle) or Tmx (+Tmx). One week later, mammary glands were harvested for analysis. **(A)** Representative fluorescent mammary gland whole mount images detecting endogenous mT and mG expression are shown for each treatment group. In vehicle-treated K8mTmG mice, mT was expressed throughout the mammary epithelium, whereas no mG expression was detected. In Tmx-treated K8mTmG mice, high levels of mG, and low levels of mT, expression were observed throughout the mammary epithelium. Scale bars: 1 mm. **(B)** MECs were isolated from vehicle-treated (n=3) and Tmx-treated (n=9) mice, and the mT- and mG-positive populations were each analyzed by FACS using CD24 and CD29 fluorescent-conjugated antibodies to separate the epithelial cells into luminal ($CD24^{hi}CD29^{lo}$) and basal ($CD24^{lo}CD29^{hi}$) cell subpopulations. FACS dot plots show the mT-positive cells from vehicle- and Tmx-treated mice are comprised of luminal and basal cells, whereas the mG-positive cells from Tmx-treated mice are mostly luminal cells. The percentages of mG-positive cells within each subpopulation are indicated on the FACS plot. **(C)** Mammary

gland sections from Tmx-treated mice (n=5) were co-stained by IF using antibodies to GFP and K8 (top three panels) or K14 (bottom three panels). Scale bars: 40 μm. A scatter plot graph shows the quantification of K8 and GFP, and K14 and GFP, co-localization, with each point representing the average from a single mammary gland. The n represents the number of glands. Quantification was performed on two glands from each mouse. The average GFP percentages in each group are indicated on the graph.

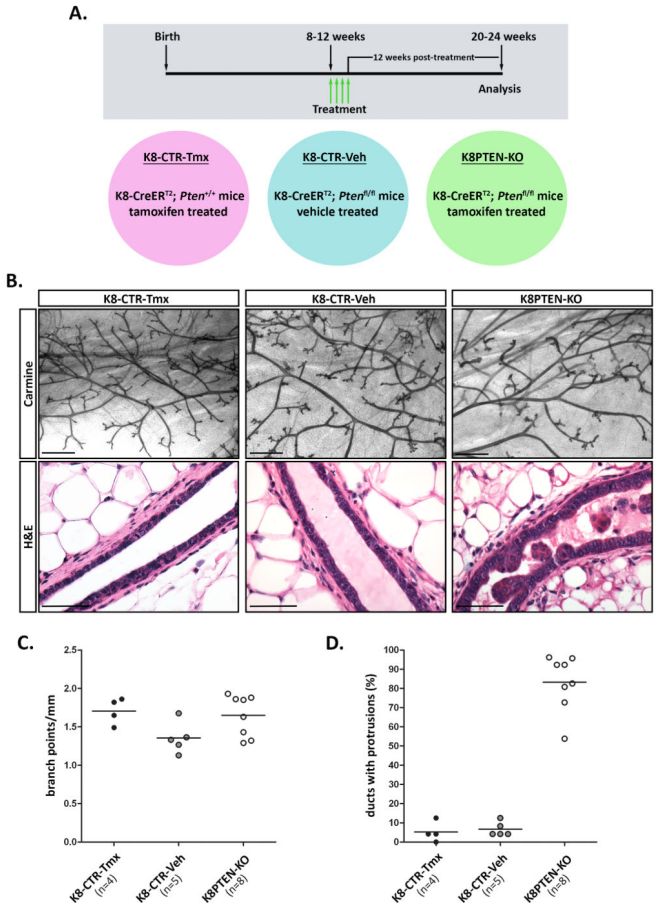

Figure 2. Luminal PTEN loss disrupts lumen maintenance and epithelial architecture within the mammary ducts

A–D) K8-CreER^{T2}; *Pten*$^{fl/fl}$ and K8-CreER^{T2}; *Pten*$^{+/+}$ mice were treated with vehicle or Tmx at 8 to 12 weeks of age to generate control (K8-CTR-Veh or K8-CTR-Tmx) or luminal epithelial *Pten*-null (K8PTEN-KO) groups, and the mammary glands were harvested 12 weeks later. **(A)** A timeline (gray box) illustrates the time of treatment (green arrows), for four consecutive days, and the time of analysis. The individual treatment groups (colored circles) are indicated below the timeline. **(B)** Representative images of carmine-stained mammary gland whole mounts illustrate similar ductal morphology between the treatment groups. Scale bars: 1 mm. Representative images of H&E stained mammary sections are shown. The control ducts exhibited single-layered epithelial compartments surrounding epithelial-free lumens, whereas the K8PTEN-KO ducts had epithelial cells protruding into the lumens. Scale bars: 50 μm. **(C)** A scatter plot graph shows that there were no significant differences in branching morphogenesis between the treatment groups. Each dot represents branching quantification from one gland from one mouse. The n represents the number of mice. **(D)** A scatter plot graph shows that more than 80% of the ducts from K8PTEN-KO mice contained protrusions, or intraluminal clusters, which was significantly higher than the amount of ductal protrusions observed in controls ($p<0.0001$). Each dot represents quantification of ductal protrusions from one gland from one mouse. The n represents the number of mice.

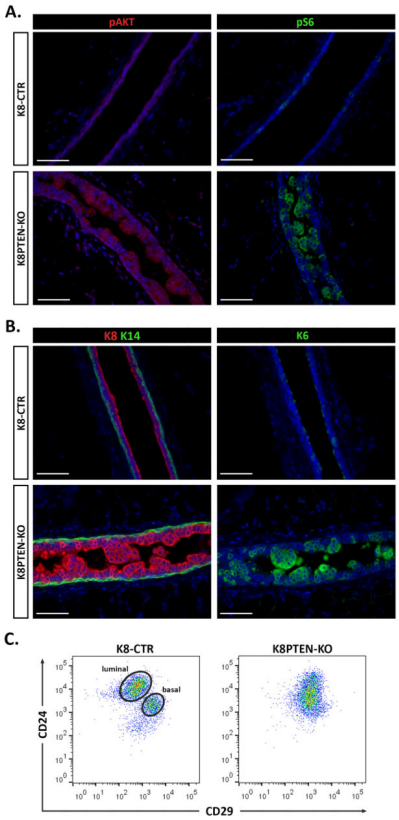

Figure 3. Luminal PTEN loss alters mammary epithelial differentiation

(A–C) K8-CreER^{T2}; *Pten*$^{fl/fl}$ and K8-CreER^{T2}; *Pten*$^{+/+}$ mice were treated with vehicle or Tmx at 8 to 12 weeks of age to generate controls (K8-CTR) or luminal epithelial *Pten*-null (K8PTEN-KO) groups, and the mammary glands were harvested 12 weeks later. **(A)** Representative IF images show high levels of the mTOR targets pAKT and pS6 in the K8PTEN-KO ducts, which are not apparent in the K8-CTR control ducts. Scale bars: 50 μm. **(B)** Representative images of IF to detect keratins 8 and 14 (K8 and K14) are shown. The K8-CTR ducts showed a single layer of luminal cells (K8-positive) surrounded by a single layer of basal cells (K14-positive), whereas the K8PTEN-KO ducts exhibited an accumulation of K8-positive cells in the lumen. Scale bars: 50 μm. **(C)** Representative FACS dot plots depict the CD24/CD29 profiles of MECs isolated from either K8-CTR (n=5) or K8PTEN-KO (n=8) mice. The MECs from K8-CTR mice sorted into the expected luminal and basal subpopulations, whereas the MECs from K8PTEN-KO mice appeared as a single population that lacked distinct subpopulations. All K8-CTR images and FACS profiles shown in this figure are from K8-CTR-Veh mice.

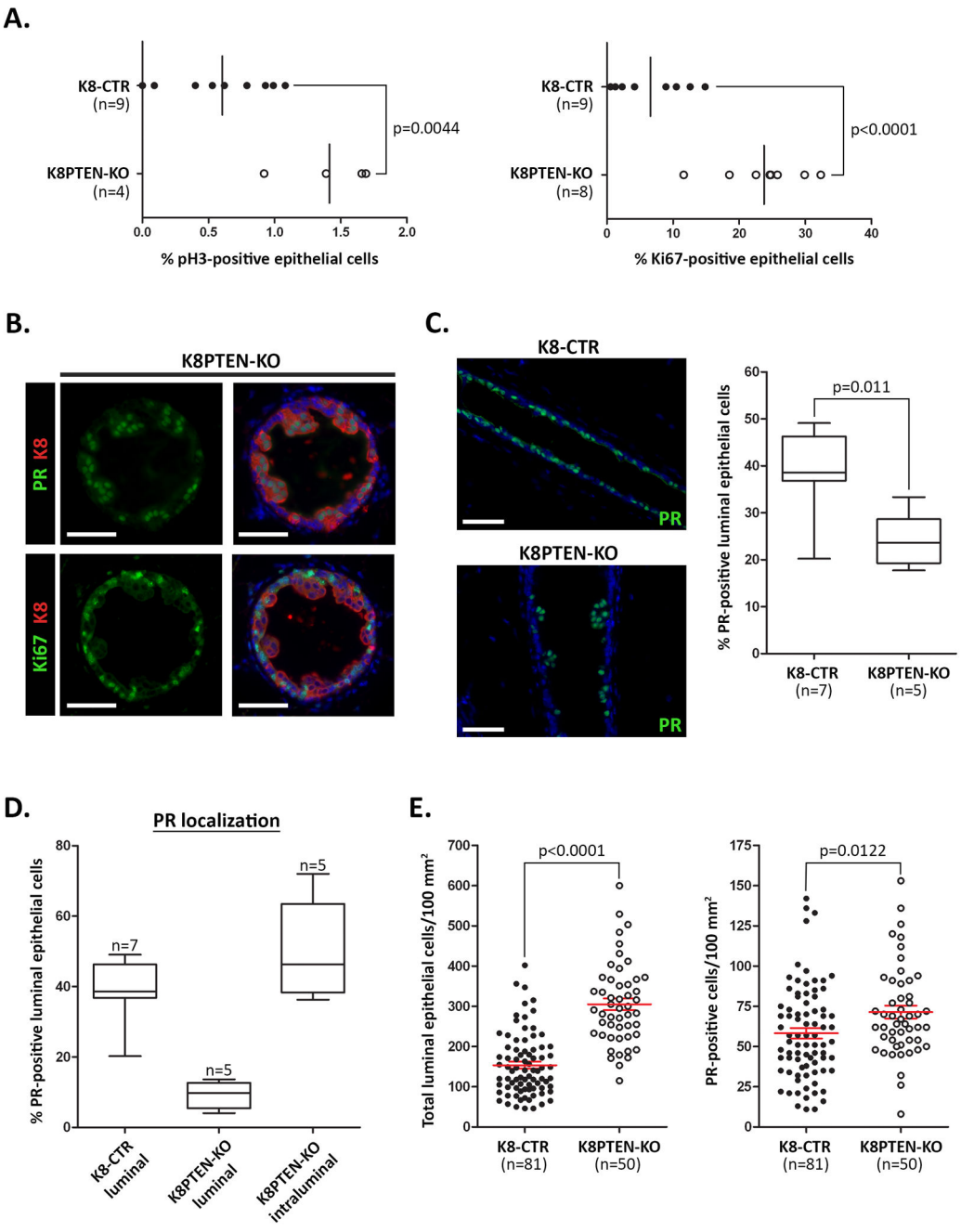

Figure 4. Luminal PTEN loss enhances proliferation, and disrupts progesterone receptor expression and patterning in the luminal epithelium

(A) IF was performed on mammary sections from K8-CTR and K8PTEN-KO mice to detect the mitotic marker pH3 and the cell cycle marker Ki67. Scatter dot plots illustrate the 2.4- and 3.6-fold increases in mitotic and actively cycling cells, respectively, in the K8PTEN-KO ducts compared with the K8-CTR ducts. The n represents the number of mice. **(B)** Representative IF images on serial mammary sections illustrate the non-overlapping, distinct localization patterns of PR and Ki67 in the K8PTEN-KO ducts. Scale bars: 50 μm. **(C)** Representative IF images depict uniform expression of PR in the luminal epithelium of the

K8-CTR ducts, whereas PR was expressed in the epithelial cells protruding into the lumen of the K8PTEN-KO ducts. Quantification of the number of PR-positive cells divided by the total number of luminal epithelial cells demonstrated a reduced percentage of PR-positive cells in the K8PTEN-KO ducts compared with the control, which is depicted in the box plot graph. The n represents the number of mice. Scale bars: 50 μm. **(D)** Quantification of PR localization showed an even greater reduction in the percentage of PR-expressing luminal cells that were directly contacting the basal epithelium in the K8PTEN-KO ducts compared with the K8-CTR ducts. Almost 50% of the intraluminal epithelial cells, those not directly contacting the basal epithelium, in the K8PTEN-KO ducts expressed PR. The n represents the number of mice. **(E)** Quantification revealed a 2-fold increase in the total number of luminal epithelial cells, which was accompanied by a 1.2-fold increase in the total number of PR-positive cells, in the K8PTEN-KO ducts compared with the K8-CTR ducts. The n represents the number of random 40× images from which the epithelial cells were counted from seven K8-CTR and five K8PTEN-KO mice. All K8-CTR images shown in this figure are from K8-CTR-Veh mice.

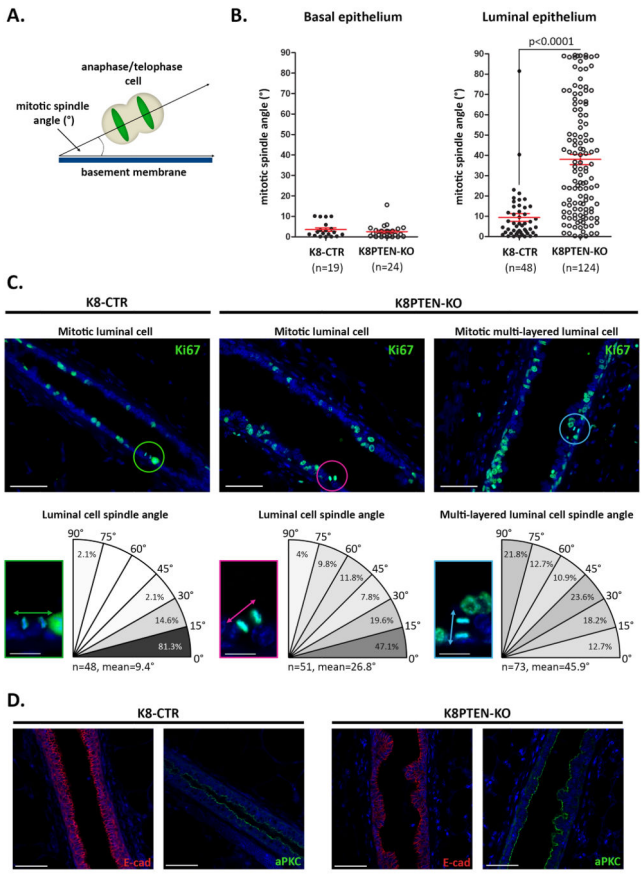

Figure 5. Luminal PTEN loss results in misoriented mitotic spindles, without altering cell-cell adhesion or apical polarity

(A–C) IF staining was performed to detect cells in anaphase (pH3) or telophase (Ki67) combined with K8 or K14 to distinguish luminal and basal cells, respectively. **(A)** Mitotic spindle angles were measured by drawing a line through the centers of the condensed chromatin of the daughter nuclei of cells in anaphase or telophase and defining it as the spindle axis. The spindle angle was measured at the intersection between the spindle axis and a line drawn parallel to the basement membrane. **(B)** Quantification of the spindle angles demonstrated that luminal PTEN loss did not alter the mitotic spindle orientation of dividing basal epithelial cells, and the majority of the divisions occurred parallel to the basement membrane (spindle angle < 15º). In the luminal epithelium, the K8PTEN-KO ducts showed a 4-fold increase in mitotic spindle angles compared with the K8-CTR ducts. The n indicates individual mitotic events. **(C)** The quantification of mitotic spindle angles was further analyzed to determine differences between single- and multi-layered luminal epithelium in the K8PTEN-KO ducts. Representative low and high magnification images show mitotic Ki67-positive luminal cells from K8-CTR (left image with green inset), single-layered K8PTEN-KO (center image with pink inset), and multi-layered K8PTEN-KO (right image with blue inset) ducts. Scale bars: 50 μm (low magnification images) and 10 μm (high magnification images). Below each set of images is their corresponding spindle angles plotted as percentages in 15º increments. In the K8-CTR ducts, 81.3% of the luminal cells showed parallel divisions, whereas in the single- and multi-layered K8PTEN-KO ducts only

47.1% and 12.7%, respectively, showed parallel divisions. The n indicates mitotic events, and the mean spindle angles are shown below each angle plot. **(D)** Representative confocal IF images depict similar staining patterns of the cell-cell adhesion marker E-cad, and the apical polarity marker aPKC, between K8-CTR and K8PTEN-KO ducts. Scale bars: 50 μm. All K8-CTR images shown in this figure are from K8-CTR-Veh mice.

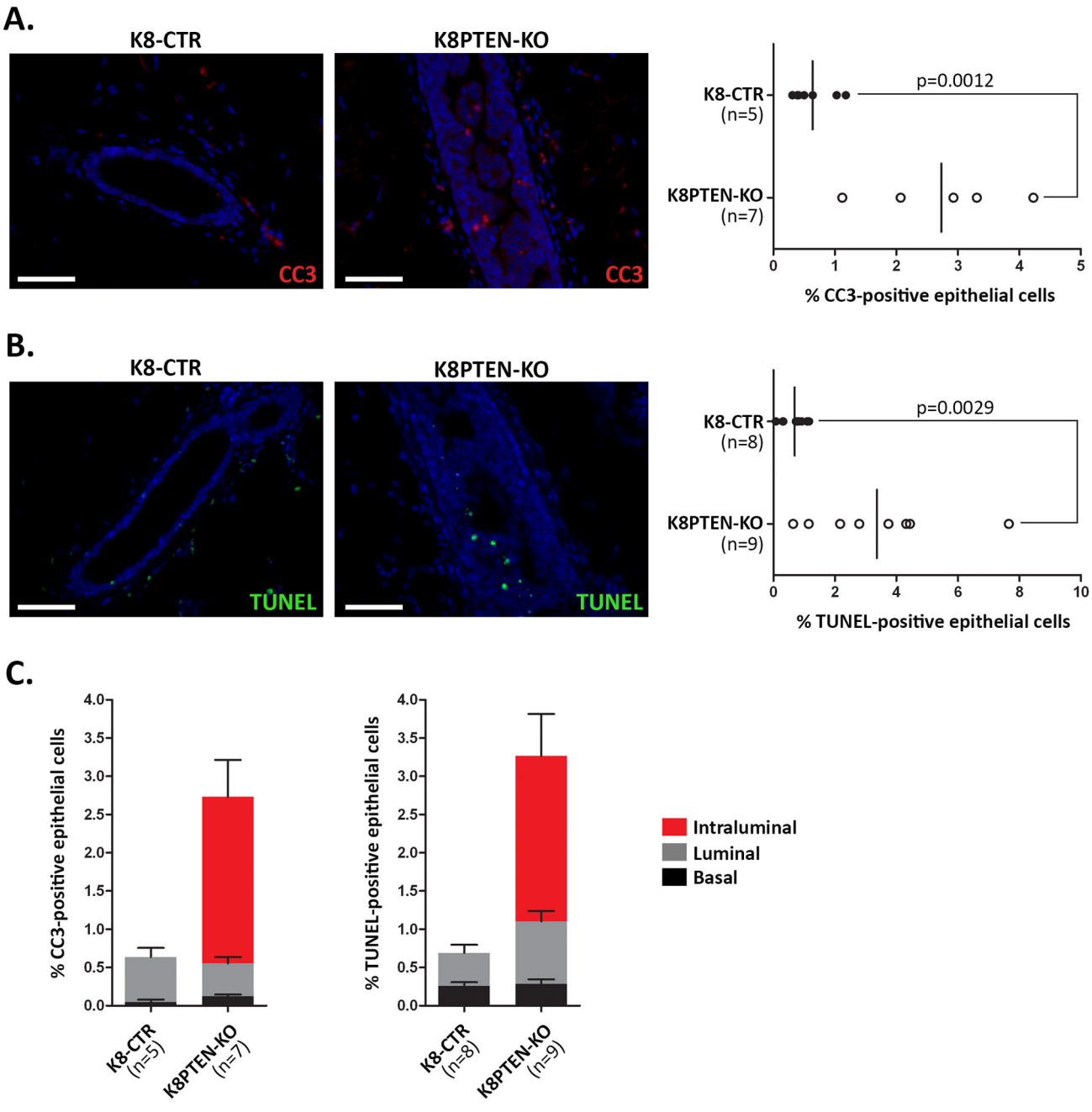

Figure 6. Intraluminal cells in K8PTEN-KO ducts show enhanced apoptosis

(A–C) To determine the levels of apoptosis, IF staining was performed to detect the apoptotic marker CC3 combined with K8, or TUNEL assays were performed. Representative IF images of CC3 **(A)** and TUNEL **(B)** show increased levels of apoptosis in the K8PTEN-KO ducts. Quantification demonstrated 4.3- and 4.9-fold increases in CC3 and TUNEL levels, respectively, in the K8PTEN-KO ducts compared with K8-CTR ducts. The n represents the number of mice. Scale bars: 50 μm. **(C)** Quantification of localization of the apoptotic cells within the ducts demonstrated that most of the increased apoptosis occurred

in the intraluminal cells of the K8PTEN-KO ducts. The n represents the number of mice. All K8-CTR images shown in this figure are from K8-CTR-Veh mice.

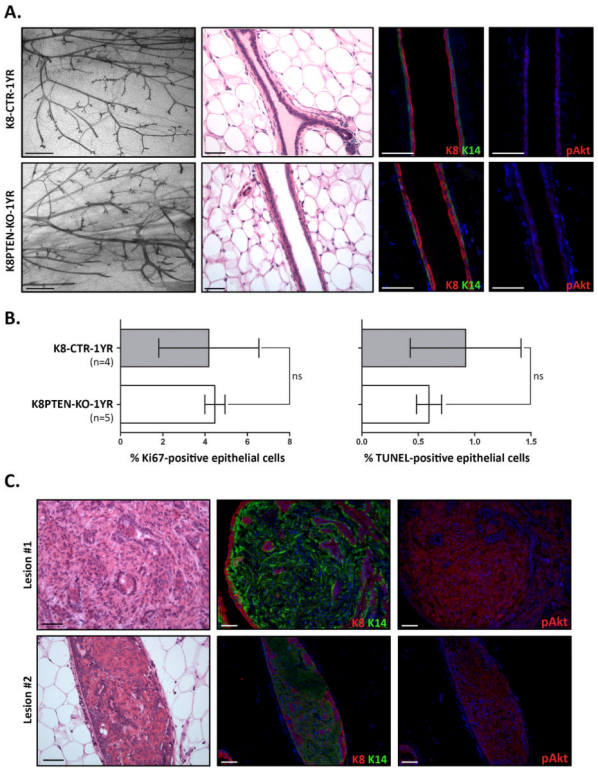

Figure 7. One year post-Tmx treatment, K8PTEN-KO-1YR ducts are similar to K8-CTR-1YR ducts and show little evidence of PTEN loss

To determine long-term effects of PTEN luminal loss, K8-CreER^{T2}; *Pten*$^{fl/fl}$ were treated with vehicle (K8-CTR-1YR) or Tmx (K8PTEN-KO-1YR) at 10 to 12 weeks of age and mammary glands were harvested 1 year later. **(A)** Representative images show similar whole mount morphology (Carmine) and ductal histology (H&E) between the two treatment groups. Scale bars: 1 mm (whole mounts) and 50 μm (H&E). Representative IF images illustrate the single-layered luminal (K8) and basal (K14) epithelial compartments in K8-CTR-1YR and K8PTEN-KO-1YR ducts. IF staining also demonstrated similar levels of pAKT between the two treatment groups. Scale bars: 50 μm. **(B)** Bar graphs depict similar levels of proliferation (Ki67) and apoptosis (TUNEL) between the K8PTEN-KO-1YR and control ducts. The n represents the number of mice. **(C)** At 1 year post-Tmx treatment, four out of five K8PTEN-KO-1YR mice had glands with single mammary lesions, whereas no lesions were detected in the glands of control mice. IF staining showed that the lesions were mostly K14 positive, and that the K14-positive cells had high levels of pAKT. Scale bars: 50 μm.